1   **Isolation and characterisation of watermelon (*Citrullus lanatus*) extracellular vesicles and**

2   **their cargo**

3   Kate Timms[a,b], Beth Holder[c], Anil Day[d], John McLaughlin[b,e,f], *Melissa Westwood[a,b],

4   *Karen Forbes[a,g]

5   [a] Maternal and Fetal Health Research Centre, School of Medical Sciences, University of

6   Manchester, St Mary's Hospital, Manchester M13 9WL, UK

7   [b] Manchester University NHS Foundation Trust, Manchester Academic Health Sciences

8   Centre, St Mary's Hospital, Manchester M13 9WL, UK

9   [c] Faculty of Medicine, Department of Metabolism, Digestion and Reproduction, Imperial

10   College London, London UK

11   [d] Division of Molecular and Cellular Function, School of Biological Sciences, University of

12   Manchester, St Mary's Hospital, Manchester M13 9WL, UK

13   [e] Division of Diabetes, Endocrinology and Gastroenterology, University of Manchester,

14   Manchester, United Kingdom

15   [f] Department of Gastroenterology, Salford Royal NHS Foundation Trust, Salford, United

16   Kingdom

17   [g] Discovery and Translational Science Department, Leeds Institute of Cardiovascular and

18   Metabolic Medicine, Faculty of Medicine and Health, University of Leeds, UK.

19   *Joint corresponding authors: k.a.forbes@leeds.ac.uk;

20   Melissa.westwood@manchester.ac.uk

21
22   **Keywords: extracellular vesicles, exosomes, plastid, multivesicular body, miRNA**
23
24

25   **Abstract**

26   Extracellular vesicles (EVs) facilitate cell-cell communication in animals and are integral

27   to many physiological and pathological processes. Evidence for the presence and

28   function of EVs in plants is limited. Here, we report that EVs derived from watermelon

29   fruit mesocarp are of similar size and morphology to the animal EV subtype known as

30   exosomes. Analysis of EV constituents revealed that watermelon EVs are negative for

31   endoplasmic reticulum markers, and that the miRNA and protein profiles differ from that

32   of watermelon mesocarp cells, suggesting that these EVs are actively synthesised and

33   are not merely cellular debris. Furthermore, we report a panel of proteins found in in

34   watermelon EVs as well as the published proteomes of grape, grapefruit, lemon and

35   *Arabidopsis thaliana* EVs that are novel potential plant EV markers. Bioinformatic

36   analyses suggest that plastids and multivesicular bodies are likely sites of biogenesis

37   for EVs from watermelon and other plants. Predicted functional roles of watermelon

38   EVs include development and metabolism, with several of their cargo molecules likely

39   to be key in regulation of fruit development and ripening. Further understanding of how

40   EVs may contribute to these processes would improve understanding of plant cell-cell

41   communication and could aid in the harnessing of plant EVs for greater temporal

42   control of crop development/ripening for the agricultural and retail industries.

43   **Main**

44   An ever-growing literature emphasises the critical role played by extracellular vesicles

45   (EVs) in mediating cell-cell communication, both in health and disease, in the bacterial,

46   fungal and animal kingdoms[1,2]. These EVs travel in the extracellular environment

47   before internalisation by recipient cells, delivering their cargo and altering cell function[3-

48   5]. Whilst EV-like particles have been observed in plants [6-16], their identity as true EVs

49   (i.e., vesicles that are actively secreted, rather than mere cellular fragments) is yet to be

50   confirmed. The term 'EVs' encapsulates several classes of cellular-derived vesicles

51   with varying size, composition and function. One of most studied classes of mammalian

52   EVs are exosomes, which are derived from membrane invagination in the late

53   endosomes known as multivesicular bodies (MVBs)[17,18]. Exosomes are generally

54   considered to be 50-150nm EVs that contain a range of cargo molecules, including

55   proteins, messenger RNAs (mRNAs) and microRNAs (miRNAs), which are actively

56   sorted into exosomes during exosome formation, resulting in a differing cargo profile to

57   that of the cell of origin[5,19-24]. Differing cell and EV cargo demonstrates that EVs are

58   purposeful and energy demanding cell-cell signals, not just passive cellular products.

59   Microvesicles are larger (100nm-1µm) EVs which bud directly from the plasma

60   membrane[25], meaning that their contents more closely resemble that of the donor cell.

61   The third major EV subtype is the 1-2µm apoptotic bodies, which bleb off the plasma

62   membrane in apoptotic cells[26,27] and can contain whole organelles or nuclear

63   fragments[28].

64   In plants, MVB fusion with the plasma membrane at sites of infection has been

65   observed using electron microscopy (EM), and is thought to be involved in the

66   response to pathogens[29]. Plant EVs have been shown to contain small RNAs[30], such

67   as miRNAs, which are suggested to suppress virulence genes in fungal pathogens[31,32].

68   Despite these more recent studies, majority of the studies reporting EV-like particles in

69   plants[6-16] have focused on dietary ingestion of plant EVs by animals, meaning that the

70   particles described in such studies have been characterised largely in the context of

71   their impact on mammalian cells, rather than the plant they originated from[8,11,13]. Initial

72   reports on the presence of membrane phospholipids in plant extracellular fluid[33,34] were

73   followed by a study aiming to determine whether these lipids were within EVs [15]. Using

74   the classical differential ultracentrifugation method of EV isolation followed by EM, EV-

75   like particles were visualised in pellets from apoplastic fluid at both 40,000xg and

76   100,000xg[15,35]. In keeping with their potential identity as EVs, these particles were

3

77   found to contain at least a limited protein cargo. Further characterisation of the

78   components, biogenesis and function of plant EVs has yet to be performed.

79   Determining the origin and function of plant EVs is essential to understanding plant cell-

80   to-cell communication, not only to increase fundamental knowledge of plant physiology,

81   but in understanding how these processes may be beneficially manipulated.

82   Watermelon fruits (*Citrullus lanatus*) contain an abundance of extracellular fluid and

83   have, at ripeness, a delicate mesocarp, allowing for the isolation of large quantities of

84   extracellular fluid without risk of disrupting cells and creating cellular fragments which

85   could erroneously be identified as EVs. As such, watermelon fruit is an ideal model for

86   plant EV characterisation. Here, we show that watermelon fruit contains EVs – likely

87   originating from plastids and MVB – which differ in miRNA and protein profiles to

88   mesocarp cells. Furthermore, we identify a panel of potential plant-specific EV markers

89   and predict that watermelon EVs have likely roles in sugar metabolism and fruit

90   development/ripening.

91   **Results**

92   **Characterisation of extracellular vesicles from watermelon fruit mesocarp**

93   Sequential ultracentrifugation was used to isolate EVs from watermelon mesocarp.

94   Parallel isolation from culture medium conditioned by human epithelial cells was

95   performed to validate the isolation procedure. The presence of authenticated human

96   EV markers[36-39] (ALIX^{+ve}/CD63^{+ve}/CANX^{-ve}; Figure 1a) in the EVs from human epithelial

97   cell conditioned media confirmed the suitability of our approach. Nanoparticle tracking

98   analysis and transmission electron microscopy revealed that watermelon and human

99   EVs have a similar morphology (Figure 1b) and size (117nm ± 14.61 Vs 129nm ± 28

100   respectively, p=0.68; Figure 1b). However, it should be noted that the watermelon EVs

101

102
103
104
105
106
107
108
109
110
111
112
113
114
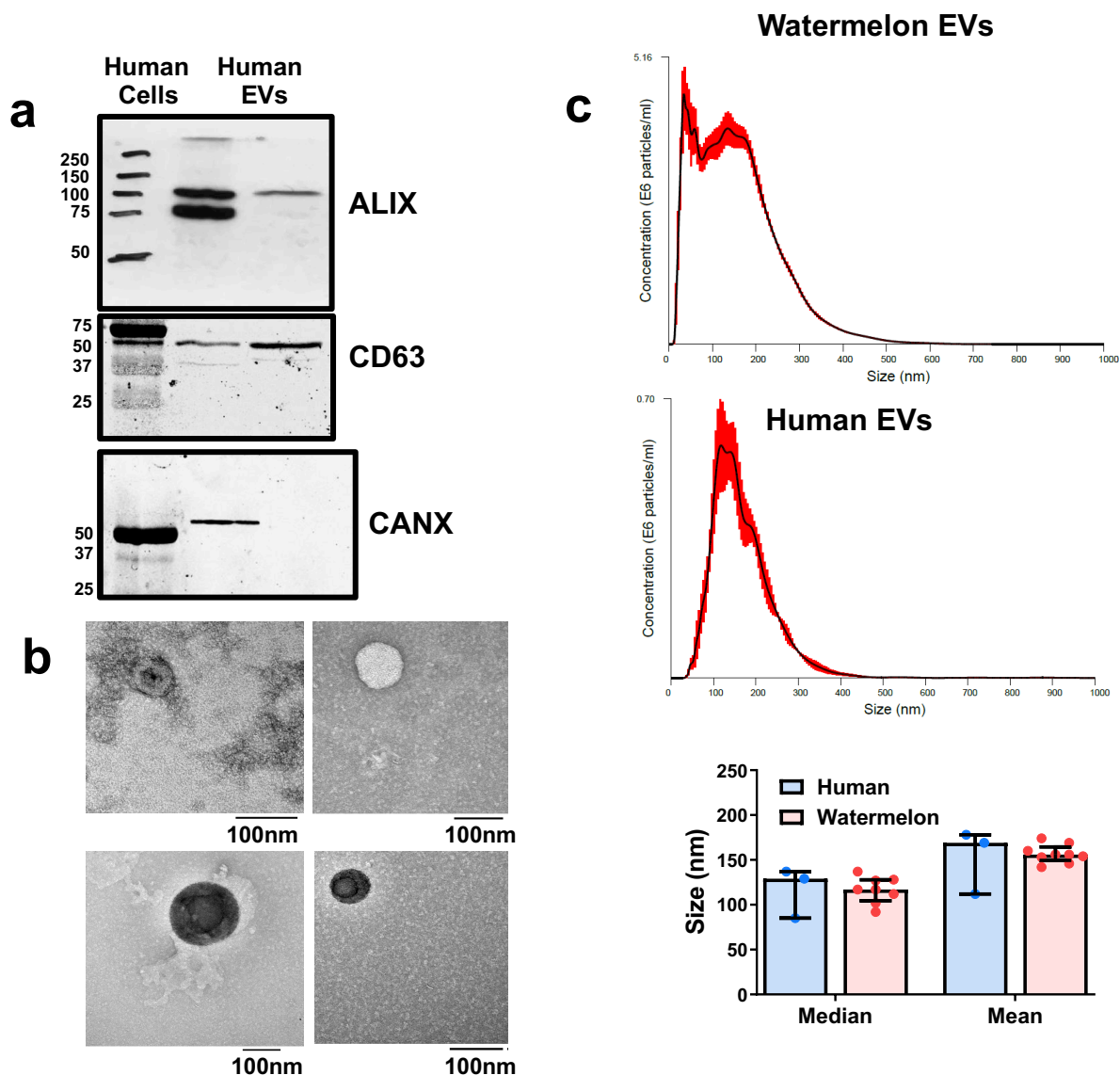115
116
117

a

b

118

Figure 1. Watermelon extracellular vesicles (EVs) resemble human exosomes. a,
Western blot analysis of positive (ALIX and CD63) and negative (CANX) markers for
exosomes in EVs isolated by differential ultracentrifugation from the conditioned media
of human Caco-2 cells. **b**, Watermelon EVs display vesicular morphology reminiscent
of human exosomes when analysed using transmission electron microscopy. EVs show
characteristic cup-shaped morphology. **c**, Size comparison of watermelon and human
derived EVs. Particles isolated by ultracentrifugation from watermelon mesocarp and
human Caco-2 cell conditioned culture media were subjected to nanoparticle tracking
analysis to determine size. Representative size distribution graph for watermelon EVs
(n=8) and human EVs (n=3) for both mean (p= 0.6364) and median size (p= 0.6788)
are shown. Data are shown as median ± IQR. (n=3-8; Mann-Whitney test).

5

130 isolated here appear to consist of 2 subsets, one with a peak around 40-60nm in

131 diameter and one around 150nm, potentially reflecting two distinct subtypes of EVs.

132 The average yield of watermelon EVs was $1.85 \times 10^{10} \pm 1.63 \times 10^{10}$ EVs/ml of watermelon

133 juice. On average, the DNA yield was $2.12 \times 10^{12} \pm 9.57 \times 10^{11}$, the RNA yield was

134 $7.64 \times 10^8 \pm 9.31 \times 10^8$ particles/ng RNA and the protein yield was $1.94 \times 10^9 \pm 7.14 \times 10^8$

135 particles/µg protein. Relative to the starting volume of juice, the EV DNA yield was 0.38

136 $\pm$ 0.11 µg/ml, the EV RNA yield was 3.45 ± 1.70 µg/ml and the EV protein yield was

137 96.79 ± 32.6 ng/ml.

138 **Protein and miRNA profiling of watermelon EVs**

139 Next, to rule out the possibility that the isolated watermelon EVs were merely products

140 of cellular disruption or breakdown, we compared their protein and miRNA content to

141 that of their parent mesocarp cells. The full list of proteins identified (1838) in

142 watermelon EVs and cells is available in Supplementary table S1. 28.13% of proteins

143 were enriched and 34.98% were depleted by >1.5-fold in EVs compared to parent cells.

144 Of note, a number of cell compartment markers for the endoplasmic reticulum (ER),

145 mitochondria, nucleus and chloroplast, including established negative markers of

146 mammalian EVs such as ER-localised calnexin and nuclear-localised histone 2B, are

147 depleted in EVs compared to cells (Table 1). Principal component analysis and

148 hierarchical clustering analysis indicated that the profile of proteins in watermelon

149 mesocarp EVs differed from that of cells, though the profile varied between different

150 watermelons (Figure 2a-b). Further analysis of watermelon EV content was performed

151 by profiling the miRNAs. This demonstrated that 25.00% and 35.71% were >1.5-fold

152 enriched and depleted respectively in EVs compared to mesocarp cells (Figure 2c-e;

153 full results in Supplementary table 2). Principal component analysis confirmed that EVs

154 have a distinct profile of miRNAs compared to their parent cells (Figure 2c).

6

Cellular Compartment	Accession	Protein Name	Relative abundance in Watermelon Cells	Relative abundance in Watermelon EVs
Nucleus	Cla019920	Histone H2A	1.33	0.34
	Cla001861	Histone H2B	2.334	0.34
	Cla015219	Histone H3 expressed	1.34	0
	Cla005035	Histone H4	4.34	0.67
Endoplasmic Reticulum	Cla002648	Calnexin	7.34	0.33
	Cla013928	Protein disulfide isomerase	11.83	7.33
	Cla005127	Cytochrome P450	2.67	0.00
Mitochondria	Cla000734	Cytochrome c1	4	0
	Cla016943	Cytochrome C-2	1.00	0.34
	Cla022586	Mitochondrial ADP/ATP carrier protein 3	8.34	1.67
	Cla002230	Mitochondrial ADP/ATP carrier protein 1	2.67	0
Chloroplast	Cla010898	Phytoene desaturase	7	2.67
	Cla006309	Sulfite reductase	5	0.34
	Cla008831	Plastid lipid-associated protein 3, chloroplastic	1.67	0.67
	Cla000424	Chloroplast outer envelope protein 37	2	1.67
	Cla020214	Zeaxanthin epoxidase chloroplastic	1	0
	Cla008113	Tic110 family transporter chloroplast inner envelope protein	4.33	1

155

Table 1: Depletion of cell compartment markers in watermelon extracellular vesicles (EVs) in comparison to watermelon cells.
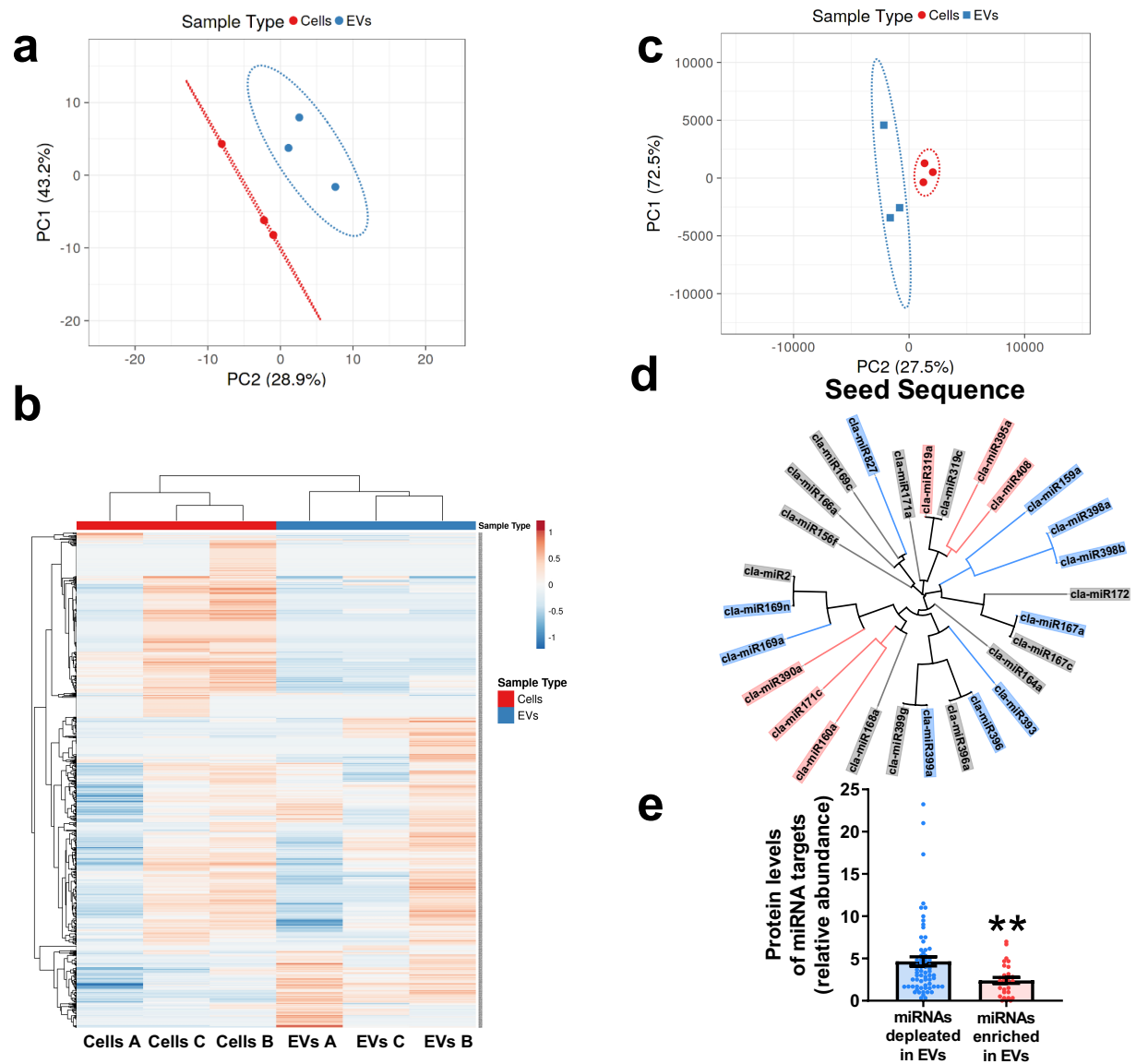
158

159

Figure 2: Characterisation of the watermelon extracellular vesicle (EV) proteins and miRNAs. a-b The proteome of watermelon mesocarp EVs differs from that of cells. Watermelon protein profiles (n=3) were analysed using principal component analysis (**a**; PCA; log10(relative abundance)) or hierarchical clustering (**b**). **c-e**, miRNAs with a 1.5-fold higher/lower level in EVs than in cells were designated as enriched/depleted (n=3). **c**, PCA of miRNA levels in mesocarp cells and EVs (log10($\Delta\Delta$Ct)). **d**, miRNA relationship based upon 8-base seed sequences, coloured for enrichment (red), depletion (blue) or neutral (grey) localisation in EVs with respect to cells. **e**, Protein levels of mRNAs targeted by miRNAs are enriched (n=29) or depleted (n=67) in EVs. Data are shown as mean ± SEM (Mann-Whitney test; p= 0.0045; ** = p<0.01).

179 Together these data suggest that the EVs isolated in this study are not merely

180 fragments of organelles produced during cellular breakdown or EV isolation.

181 The enrichment of specific miRNAs in watermelon EVs compared to cells suggests

182 active sorting of miRNAs in watermelon. In mammals, miRNAs are actively sorted into

183 EVs, in a sequence-dependent manner, by hnRNPA2B1[23]. To determine whether the

184 same may be true of plant EVs, a BLAST search for hnRNPA2B1 was conducted. No

185 sufficiently orthologous protein was found in the Viridiplantae kingdom. Furthermore,

186 analysis of the relationship between miRNA sequence, sequence motif or secondary

187 structure and enrichment/depletion in watermelon EVs (data not shown) revealed no

188 obvious association. However, when the miRNA seed sequence was considered in

189 isolation, it did appear that some related seed sequences were similarly regulated

190 (Figure 2d). As the seed sequence of miRNAs is the most important region for miRNA-

191 mRNA binding, and mRNA abundance is inversely linked to miRNA sorting EVs in

192 animals[40], we hypothesised the relationship between seed sequence and EV

193 enrichment may relate to the abundance of target mRNAs within watermelon cells.

194 Whilst the levels of mRNAs in watermelon cells are unknown, our analysis of the

195 proteins present in watermelon cells and EVs can be used as a proxy measure of the

196 abundance of their mRNAs; our data show that the levels of the cellular proteins that

197 are the targets of miRNAs enriched in EVs were lower than those that are the targets of

198 miRNAs depleted in EVs (Figure 2e; $p<0.01$). A full list of watermelon EV miRNA

199 targets is given in Supplementary Table 3.

200 **Identification of potential plant EV markers**

201 There is a growing consensus on the use of several lipid-associated/membrane-

202 spanning and cytosolic proteins as suitable markers of mammalian EVs[39]. Likewise,

203 there is a proposed range of 'negative markers to distinguish human EVs, particularly

204   the MVB derived exosomes, from cellular debris[39]. We also demonstrated the depletion

205   of some of these 'negative' markers, such as calnexin, in watermelon EVs compared to

206   watermelon cells (Table 1).

207   Currently, there are no widely recognised positive markers of plant EVs and there are

208   no sufficient homologs of human markers present in the watermelon proteome,

209   suggesting mechanisms of biosynthesis may differ. To discover potential novel

210   marker(s) of plant EVs, the proteomes of EVs from watermelon and EV-like particles

211   previously isolated from grape[11], grapefruit[13], lemon[14] and *Arabidopsis thaliana*[6] were

212   compared (Table 2). One protein, enolase, is present in the EVs of all 5 species and,

213   interestingly, is the second most commonly reported protein in human EVs[41]. Of the 15

214   remaining potential markers with a human ortholog, all have been identified in human

215   EVs and 11 are within the top 250 most commonly identified human EV proteins[42].

216   **Plastids and multivesicular bodies are likely sites of watermelon extracellular vesicle**

217   **biogenesis**

218   We next interrogated the EV protein profile using gene ontology (GO) enrichment

219   analysis, reasoning that such information might help to identify the site of EV

220   biogenesis. This indicated that the majority of the EV proteins are from either the

221   cytoplasm or the plastid and its derivatives (Figure 3a). The plastid is a known site of

222   vesicles[43-49] approximating the size of the smaller peak identified in nanoparticle

223   tracking analysis of watermelon EVs (Figure 1c), making the plastid a credible

224   candidate site for plant EV biogenesis. Further prediction based on cellular localisation

225   signals and comparison of the watermelon EV proteome with previously published

226   data[50] supports this hypothesis, with 73.58% of watermelon EV proteins

227   predicted/observed to be within plastids (Figure 3b). The same high percentage of

228   plastid proteins was seen in other plant species for which data was available.

Accession	Protein name	Fold regulation in watermelon EVs compared to watermelon cells	No. plant species identified in (Max. 5)	Within top 250 human EV proteins? (N/A indicates no human ortholog)
Cla001345	Vesicle-associated protein 4-2	Only detected in EVs	4	N/A
Cla020983	Vesicle-associated membrane protein 7C	+11	4	No
Cla023344	Sodium/calcium exchanger family protein	+6	4	No
Cla016803	Profilin	+5	4	Yes
Cla017822	V-type proton ATPase subunit G	+3.17	4	Yes
Cla018715	Outer membrane lipoprotein Blc	+2.75	4	N/A
Cla012175	Triosephosphate isomerase	+2.31	4	Yes
Cla010547	Adenosylhomocysteinase	+2.09	4	Yes
Cla019014	Enolase	+2.01	5	Yes
Cla011437	Aquaporin 1	+2	4	No
Cla007587	Malate dehydrogenase	+1.63	4	Yes
Cla012184	Pyrophosphate-energized vacuolar membrane proton pump family protein	+1.54	4	N/A
Cla019719	Tubulin beta chain	+1.41	4	Yes
Cla015847	Peptidyl-prolyl cis-trans isomerase	+1.31	4	Yes
Cla007792	Actin	+1.07	4	Yes
Cla023447	Catalase	-1.7	4	No
Cla005204	Heat shock protein 90	-2.26	4	Yes
Cla012806	Nucleoside diphosphate kinase	-13.99	4	Yes

229

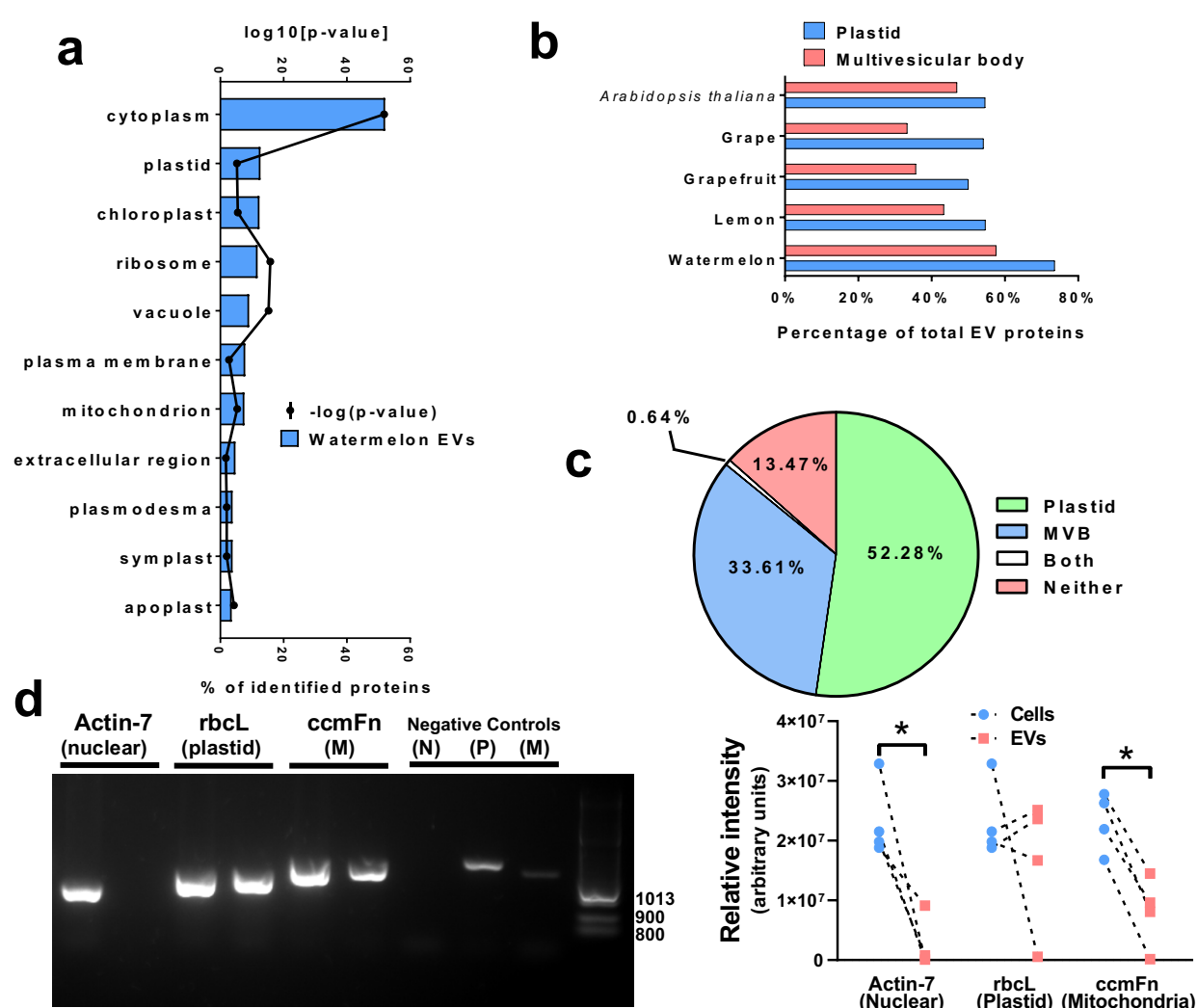230 **Table 2: Candidate plant extracellular vesicle markers.**

231

Figure 3: Watermelon EVs are likely derived from plastids and multivesicular bodies. a, GO enrichment of watermelon EV protein localisation (Bonferroni p-value correction). **b,** Comparison of the percentage of multivesicular body (MVB) and plastid proteins present in EVs from watermelon and those previously published for EVs in lemon[14], grapefruit[13], grape[11] and *Arabidopsis thaliana*[6] were aligned to the proteomes of watermelon chromoplasts[50] and Arabidopsis thaliana multivesicular bodies[51]. **c**, A comparison of the percentage of the total watermelon EV protein mass predicted and/or reported to reside cellularly within plastids, MVB, both or neither organelle. **d**, Relative quantification of DNA of nuclear (N; actin-7; p=0.0286), plastid (P; rbcL; p= 0.6857) and mitochondrial (M; ccmFn; p= 0.0286) origin in EVs compared to cells (n=4). Data are shown as median (Mann-Whitney test; * = p<0.05).

261 Furthermore, the yellow-orange colouration of watermelon EV pellets suggests the

262 presence of lycopene, which is produced and stored within watermelon chromoplasts.

263 Interestingly, our analysis of the published proteomes of EV-like particles isolated from

264 grape[11], grapefruit[13], lemon[14] *and Arabidopsis thaliana*[6] suggests that plastids might be

265 a common site of EV synthesis in plants (Figure 3b).

266 Animal exosomes originate from MVB. As neither GO enrichment nor predictive

267 localisation based upon sequence are equipped for the assessment of MVB proteins,

268 BLAST was used to align the proteome of EVs from watermelon, grape, grapefruit,

269 lemon and *Arabidopsis thaliana* to that of *Arabidopsis thaliana* MVB[51]. This revealed

270 that the majority of the non-plastid EV proteins are present in plant MVB, with some

271 proteins being present in both organelles (Figure 3b). When protein abundance is

272 considered, rather than the number of individual proteins, 52.28% of all protein mass in

273 watermelon EVs is from proteins which reside solely in plastids, whilst proteins residing

274 solely in MVB account for just 33.61% of the total protein mass in watermelon EVs

275 (Figure 3c), suggesting that EVs of potential plastid origin may be more abundant than

276 those of MVB origin.

277 Proteins are not the only plastid component present in EVs. Whilst DNA of nuclear

278 (actin-7) and mitochondrial (ORF204) origin are depleted in EVs compared to cells

279 (Figure 3d; $p < 0.05$), the level of plastid DNA (rbcL) in cells and EVs was similar. The

280 level of plastid DNA present in EVs varied between watermelons. Nonetheless, these

281 data further support a plastid origin for at least a subset of watermelon EVs.

282 **Predicted roles for watermelon extracellular vesicles in fruit development/ripening**

283 Next, we turned to predicting the potential roles of watermelon EVs by examining GO

284 cellular process and pathway enrichment for EV proteins and miRNA targets. The

285 targets of miRNAs that are enriched in cells appear to be concerned mainly with the

13

286   various processes of cellular metabolism (Figure 4; blue), whereas the targets of

287   miRNAs enriched in watermelon EVs are primarily involved in processes of

288   development and reproduction (Figure 4; red). Analysis of the proteins enriched in

289   watermelon cells and EVs suggests that they have broadly similar roles in both

290   compartments (Figure 5a). However, whilst the processes and pathways of proteins

291   enriched in cells cover a wide range of cellular metabolic processes, those for proteins

292   enriched in EVs focus on nucleic acid metabolism, suggesting a role in gene

293   expression. When considered in isolation, those watermelon EV proteins that are

294   predicted to usually localise to the MVB or the plastid are also mostly involved in

295   metabolism (Figure 5b). The second highest enriched biological process theme in MVB

296   is gene expression (11.1%), with nucleic acid metabolism also featuring in the

297   metabolism processes. However, in plastids, the second highest enriched biological

298   process theme is response to reactive oxygen species (4.61%), followed closely by cell

299   signalling (4.15%), and gene expression does not feature. These data suggest distinct

300   roles for the proposed MVB-derived and plastid-derived EV subtypes.

301   As development/reproduction, metabolism and control of reactive oxygen species are

302   all important for fruit production and ripening, we hypothesised that watermelon EVs

303   could have a role in these processes. We therefore analysed an open access dataset[52]

304   of the transcripts expressed in the fruit flesh of the LSW177 variety of watermelon on

305   days 10-34 after pollination, predicting that the mRNA targets of miRNA found in

306   watermelon EVs would be downregulated over time if EVs truly influence fruit

307   development/ripening. The data presented in Figure 6 support this hypothesis as the

308   levels of watermelon EV miRNA targets decrease across the timescale of fruit

309   development and ripening, reaching significantly lower expression than the average of

310   all watermelon transcripts at day 34 (p<0.0001) when the fruit is considered ripe.
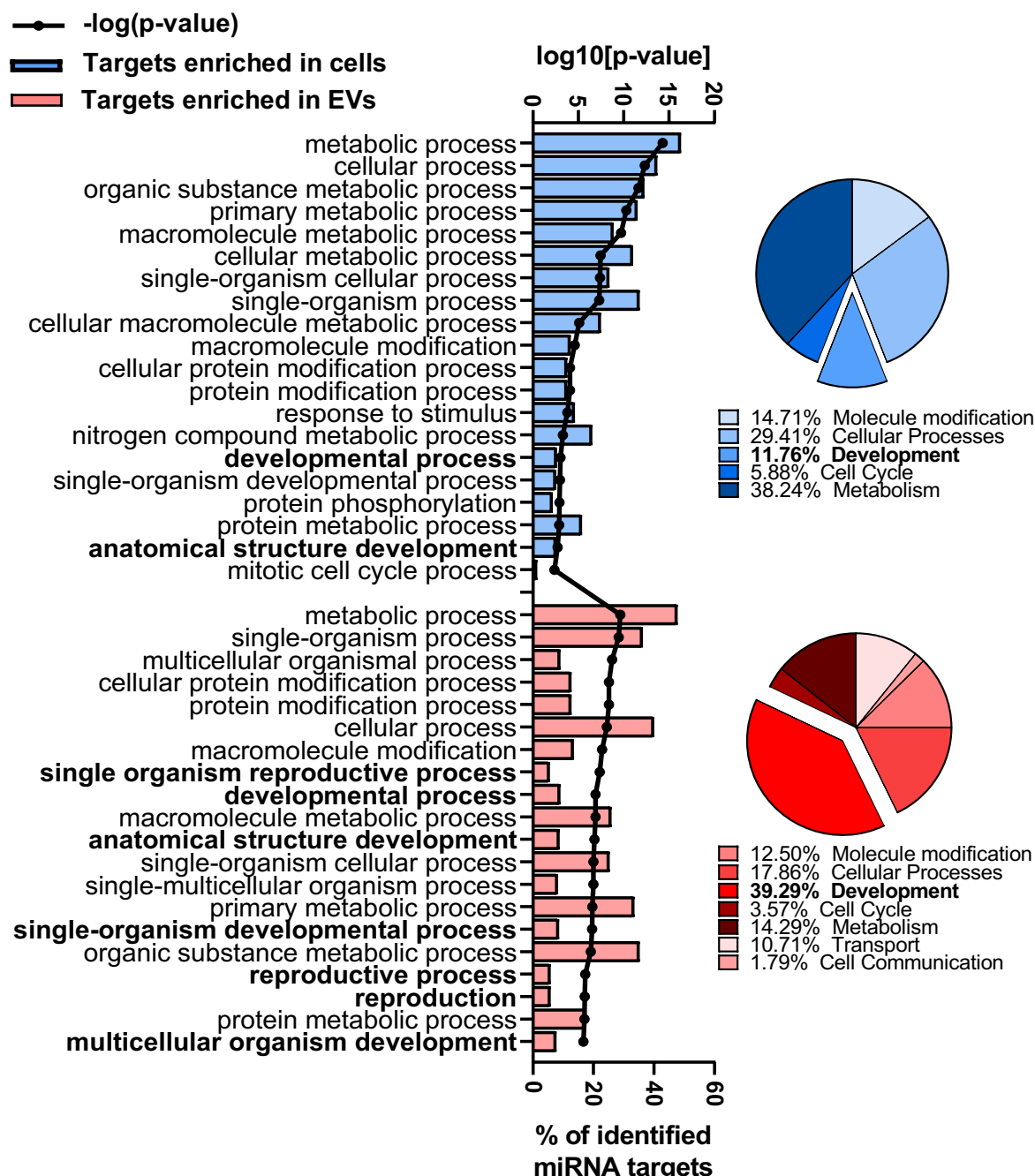
14

Figure 4: A potential role for watermelon EVs miRNAs in fruit development/ripening. Functions of miRNAs (via their predicted mRNA targets) which are enriched in watermelon cells (blue) or EVs (red) were predicted through GO biological process enrichment analysis. Top biological processes based upon p-value are given in the bar chart and all processes grouped by theme given in the pie charts (development emphasised). p-value correction for multiple testing was preformed using the Bonferroni method.
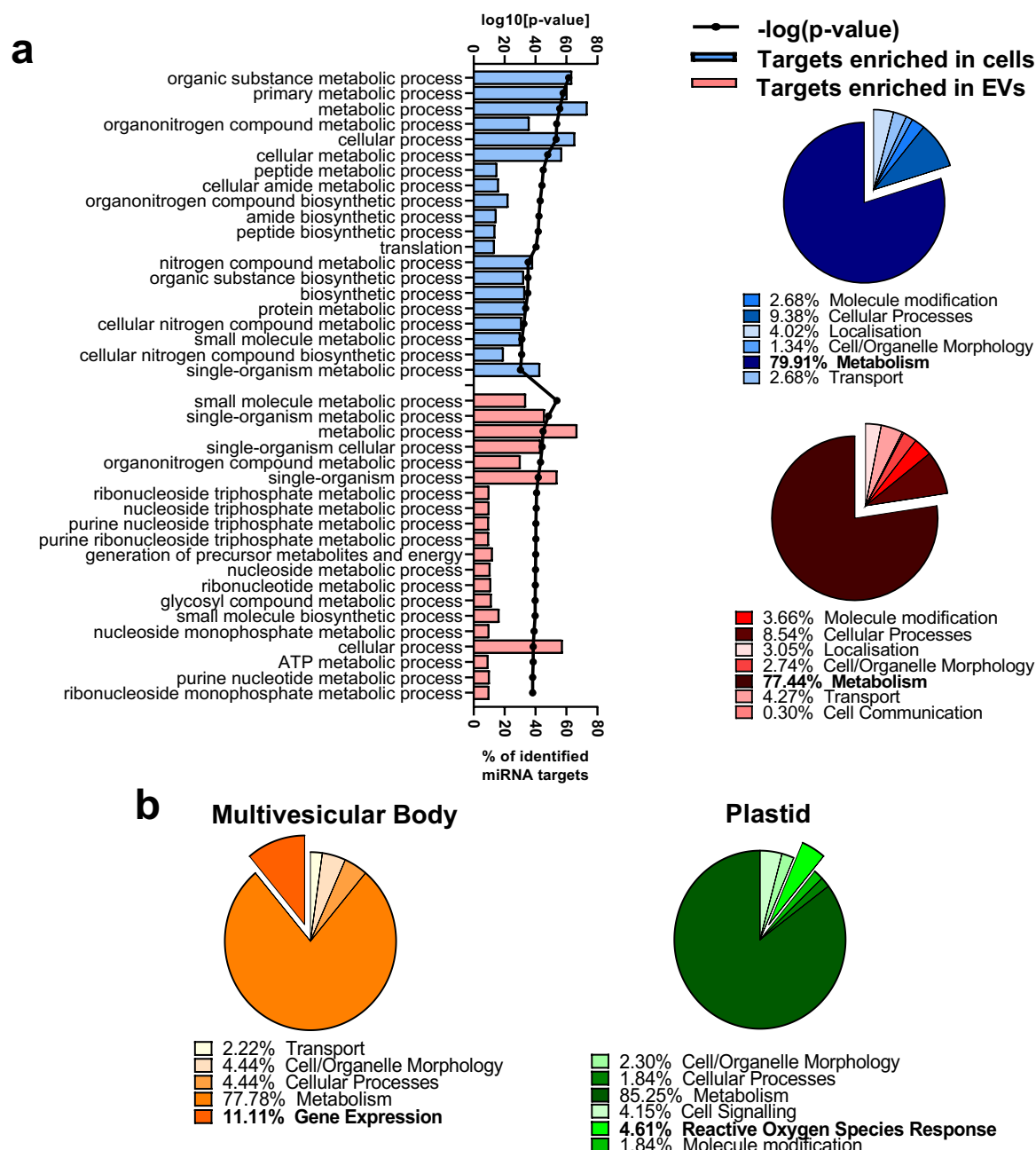
15

Figure 5: A potential role for watermelon EV proteins in metabolism, gene expression and reactive oxygen species degradation. a, Functions of proteins which are enriched in watermelon cells (blue) or EVs (red) were predicted through GO biological process enrichment analysis (Bonferroni p-value correction). The most significantly enriched biological processes are given in the bar chart and theme-grouped processes in the pie charts (metabolism emphasised). **b,** Biological process enrichment for watermelon EV proteins predicted to localise to the multivesicular body or plastid. The top biological process theme following from metabolism is emphasised.

16
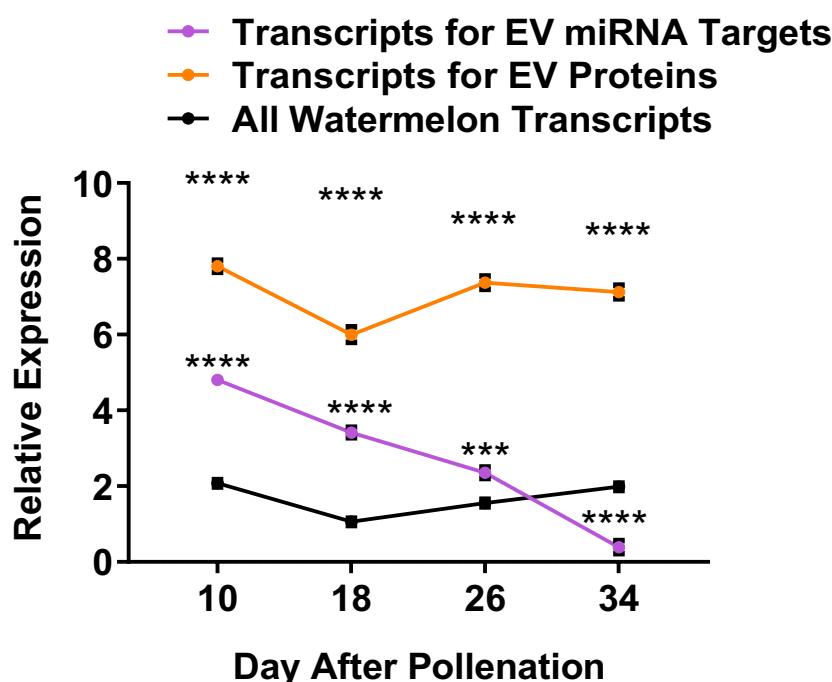
Figure 6: Dynamic changes in watermelon EV miRNA and protein levels across fruit ripening. Levels of miRNA target mRNA and the mRNA for proteins found in watermelon EVs were mapped to mRNA levels across watermelon ripening using a publicly available transcriptomics dataset (Zhu et al., 2017). 105-2944 mRNA per datapoint, two-way ANOVA with Sidak's multiple comparisons test, comparisons are to 'all watermelon transcripts'. Data are presented as mean ± SEM.

369 Moreover, the transcripts for proteins present within watermelon EVs were enriched

370 compared to all watermelon transcripts across this entire period.

371 **Discussion**

372 Here we present the first data on the isolation and characterisation of EVs from

373 watermelon fruit. These EVs are of a size and morphology reminiscent of animal

374 exosomes[53]. We have also reported the average yield of watermelon EVs per millilitre

375 of starting juice and the ratio of particles to DNA, RNA and protein. These

376 characterisations are a first in the plant EV field and are crucial for ensuring that plant

377 EV studies are executed to the same standard as is expected in the mammalian EV

378 field. The particle/protein ratio of 1.85×10^{10} particles/µg protein is considered to be

379 highly pure[54], suggesting that the methodology presented here is sufficient to isolate

380 EVs from watermelon which are free of protein contamination. However, analysis of

381 other potential contaminant molecules which may be present in watermelon juice, such

382 as glucose and sucrose, is not currently known.

383 Human exosomes exhibit miRNA[5] and protein[38] profiles that differ from their cells of

384 origin due to active loading of cargo, a phenomenon we also observed in watermelon

385 EVs. In watermelon EVs, miRNA sorting appears to be associated with abundance of

386 cellular target proteins; high levels of cytoplasmic mRNA may sequester miRNA away

387 from the site of EV biogenesis, as has been previously identified in humans[40].

388 However, we acknowledge that protein levels are skewed by post-transcriptional

389 regulation and are therefore an imperfect proxy of mRNA levels. Whilst we did not

390 observe any discriminating sequence or structural motifs between enriched and non-

391 enriched miRNAs in watermelon EVs, characterisation of the full complement of cellular

392 and EV miRNAs is required before this can be confirmed.

393   Several studies have described EVs or EV-like particles isolated from plants using

394   broadly similar methods to those we employed in this current study[6-15]. Some report

395   vesicles larger than human exosomes and watermelon EVs[8,9,11], potentially due to

396   vigorous isolation techniques (i.e. prolonged blending) resulting in cellular debris.

397   However, it is also possible that some plant EVs may be constitutively larger, perhaps

398   due to differences in biogenesis. One of the main determinants of the size of vesicles

399   isolated by ultracentrifugation is the final pelleting force[55]. Whilst most studies have

400   pelleted plant EV-like particles at standard forces of 100,000-150,000xg, two studies

401   reported the isolation of EVs at just 40,000xg[6,15]. However, the lack of reporting on the

402   rotors or the pelleting k-factor used to isolate EVs precludes direct comparisons,

403   reinforcing the importance of standardisation in reporting EV isolation and

404   characterisation.

405   Plastids and MVB are both vesicle-containing organelles[43] and it is therefore

406   conceivable that both produce plant EVs, perhaps of distinct functionality. More than

407   half of proposed plant EV markers (i.e., those most conserved in EVs between species)

408   are present in chromoplasts, around one third in MVB and one tenth in both, supporting

409   dual origin. Whilst our hypothesis that some watermelon EVs may be generated in

410   plastids is novel, the cell-to-cell movement of plastid components through an

411   unidentified mechanism has been reported previously[56]. Movement of the whole plastid

412   genome between cells was proposed to occur through the movement of intact

413   plastids[56], but this hypothesis has been criticised due to the large size of plastids

414   relative to the diameter of the plasmodesmata channels between cells[57]. Our data

415   suggest that EVs could be responsible for the transfer of genetic material, as plastid

416   DNA is present at a relatively high abundance in watermelon EVs. DNA sequencing of

417   plant EVs would further confirm this hypothesis.

418   We have identified a number of potential plant EV marker proteins. We propose that a

419   panel of the potential plant EV markers identified herein – perhaps those with highest

420   fold-enrichment in EVs as compared with cells – be used in future plant EV studies to

421   enable better understanding of the nature of plant EVs as well as ensuring

422   standardisation amongst the field. For example, vesicle-associated protein 4-2 which

423   was identified solely in EVs and is predicted to reside solely in plastids,

424   adenosylhomocysteinase which resides solely in MVB and enolase which is predicted

425   to reside in both plastids and MVB and is also highly abundant in mammalian EVs.

426   Similarly, we recommend that 'negative' EV markers from human and animal studies be

427   extended for use in the plant field, as we have shown a number of these to be valid for

428   the characterisation of plant EVs. This includes calnexin and histone 2B.

429   Previous studies investigating EV-like vesicles in plants have focused on their role in

430   the plant response to infectious agents [29,58]. Our bioinformatic analyses suggest that

431   plant EVs may also play a role in metabolism and fruit development/ripening. We found

432   that watermelon EVs contain the machinery needed for the metabolism of sucrose and

433   glucose, such as glucose-6-phosphate isomerase and sucrose synthase, suggesting

434   that plant EVs may play a role in the accumulation and metabolism of sugar in fruits,

435   allowing for rapid tissue expansion and making fruit palatable for seed propagation by

436   animals. Growth-regulating factors (GRF) 1, 4, 5 and 9 are predicted targets of several

437   of the most abundant, if not the most enriched, watermelon EV miRNAs, including the

438   miR-396 family and miR-390-3p. GRFs are downregulated during ripening of

439   watermelon and other fruits [52,59]. A miR-396-GRF network has been implicated in the

440   size, maturation and ripening of several fruits, perhaps through influence on the

441   meristem [60-62]. Furthermore, miR-159c, which is depleted in watermelon EVs, is also

442   implicated in fruit development and ripening via its targeting of MYB33 [63,64]; this

443   transcription factor is downregulated during watermelon ripening. Overexpression of

444   miR-159 results in fruit formation in the absence of fertilisation[64,65] and downregulation

445   of miR-159 results in the production of more spherical fruit in *Arabidopsis thaliana*[66].

446   Furthermore, three miRNAs enriched (cla-miR319a, miR399g and cla-miR408) and

447   three depleted (cla-miR393, miR167a and cla-miR399a) in watermelon EVs target

448   ethylene-responsive transcription factors and ethylene producing enzymes, suggesting

449   that they may be involved in ethylene-dependent fruit ripening. Together, these data

450   suggest that watermelon EV miRNAs could be involved in the initiation and control of

451   fruit development and ripening.

452   The potential role of plant EVs in fruit ripening represents a novel finding and could,

453   with further research, aid developing technologies to manipulate this process with the

454   aim of reducing the economic burden of fruit wastage due to premature ripening and

455   subsequent spoiling of fruits before they reach the end consumer. Furthermore,

456   understanding cell-cell communication through EVs in plants could be of use in

457   agricultural grafting, aiding in the production of crops able to develop fruits/vegetables

458   in substandard environments, thereby increasing global food production. Grafted plants

459   share genetic material, with the genetic material from one individual transferring the

460   other [67-71]. Some have hypothesised that this results from whole nuclei or organelles

461   passing between the individuals following cell disruption during the grafting process

462   (reviewed in [72]). However, as mentioned above, the small size of the plasmodesmata[73]

463   communication channels between cells relative to nuclei or organelles questions the

464   feasibility of this occurring [57]. Therefore, the current prediction of a potential plastid

465   origin for watermelon EVs, especially the plastid DNA they contain, raises the

466   possibility that EVs are a vector for this genetic exchange between grafted species.

467   Further understanding of the role for EVs in grafting could, therefore, aid in increasing

468   crop yield and resilience.

469   This study contains the first detailed characterisation of plant EVs alongside exploration

470   of the potential functions of watermelon EV cargo. It is hoped that the observations and

471   suggestions made herein, including the panel of plant-specific EV markers, will enable

472   clarity and rigor in the plant EV field moving forward.

473   **Methods**

474   **Materials**

475   Unless otherwise stated, all reagents were purchased from Sigma-Aldrich.

476   **Extracellular vesicle isolation**

477   We have submitted all relevant data of our experiments to the EV-TRACK

478   knowledgebase (EV-TRACK ID: EV190074)[74].Watermelons (n=9) were purchased from

479   a range of local greengrocers and supermarkets. As the variety of watermelons is

480   usually not given in greengrocers or supermarkets, an effort was made to select

481   visually similar fruits. All were of a medium size (i.e. not described as 'giant' or 'baby')

482   and exhibited dark and light green stripes on their rind. Watermelon were from a range

483   of countries of origin and were purchased throughout the year so as to best reflect the

484   fruits available to consumers. The watermelon mesocarp was removed from the rind

485   with a knife and the weight of dissected mesocarp recorded. Dissected mesocarp was

486   pulsed for 1 second in a standard kitchen blender. This brief blending was sufficient to

487   disrupt the structure of the mesocarp, but did not break open the seeds or produce a

488   homogenate. Large tissue fragments were removed using a coarse sieve to leave an

489   opaque juice. EV isolation was then performed using differential ultracentrifugation at

490   4°C with a Sorvall Discovery 100SE centrifuge set to 'RCFavg'. Firstly, the juice was

491   centrifuged at 1,000xg for 10 minutes using the A-621 fixed-angle rotor. The

492 supernatant was then centrifuged twice at 10,000xg for 10 minutes using A-621 fixed

493 angle rotor to remove the remaining large fragments of tissue, apoptotic bodies and

494 whole organelles such as plastids. The resulting supernatant was passed through a

495 0.22μm filter (Merck Millipore) then centrifuged at 100,000xg for 90 minutes (k-factor

496 207.11) in sterile tubes using the T-1250 fixed-angle rotor. The supernatant was

497 discarded, and the pellet was resuspended in 200μl of sterile phosphate buffered saline

498 minus magnesium and calcium. EV size was determined using nanoparticle tracking

499 analysis (NTA) on a NanoSight LM10 (Malvern). Per sample, 3x60 second videos taken

500 and were analysed using the NTA 2.3 software. EV morphology was determined using

501 transmission electron microscopy following negative staining with 1% uranyl acetate.

502 Images were captured on a JEM1400 transmission electron microscope (Jeol) at 120kV

503 using a 1k CCD camera (Advanced Microscopy Techniques, Corp.). Watermelon EVs

504 were compared with those isolated using the same protocol as for watermelon EVs

505 from culture medium conditioned by Caco-2 cells (ECACC #86010202; approximately

506 1.75×10^7 cells in 50ml culture medium) for 72 hours. Culture medium comprised of

507 Dulbecco's Modified Eagle Medium (DMEM), 2mM non-essential amino acids, 4mM

508 glutamine, 100U/L penicillin, 100μg/L streptomycin and 10% (v/v) fetal bovine serum

509 (Life Technologies Ltd).

510 **miRNA analysis**

511 RNA was isolated from watermelon (n=3) EVs or matched mesocarp cells (1,000xg

512 centrifugation pellet, k-factor 50430.28) using the miRVana miRNA Isolation Kit

513 (Thermo Fisher Scientific) with the addition of the Plant RNA Isolation Aid (Thermo

514 Fisher Scientific) according to the manufacturer's instructions. Following lysis and prior

515 to RNA isolation, samples were spiked with cel-miR-39 (Qiagen) to allow for

516 normalisation of extraction efficiency. Reverse transcription was performed on 125ng of

23

517   RNA – quantified using the NanoDrop 2000c – using the miScript Plant RT kit (Qiagen).

518   Currently, no products are commercially available for the profiling of watermelon

519   miRNAs. However, the high level of miRNA homology between plant species

520   (discussed in [75]) allowed profiling of watermelon miRNAs using a rice (*Oryza sativa*)

521   qPCR array, which quantifies 84 miRNAs. cDNA samples from EVs and cells were

522   analysed using the Rice miFinder qPCR array (Qiagen). snoR10, snoR31, snoR5-1a,

523   U15 and U65-2 qPCR array housekeeping genes were constant in cells and EVs and

524   were used alongside the internal reverse transcription control and cel-miR-39 for

525   normalisation. Of the miRNAs on the array, 83 were detected. The melting temperature

526   of each miRNA was compared between qPCR array plates; a difference of 2°C or more

527   suggests that a different sequence had been amplified, such miRNAs were removed

528   from analysis (17 miRNAs). As an additional stringency measure, any rice miRNA with

529   a sequence containing >2 deviations from the published watermelon sequence (Frizzi

530   et al., 2014, Liu et al., 2013) were excluded (38 miRNAs). 28 miRNAs were taken

531   forward for further analysis.

532   **Western blot**

533   Caco-2 cells and EVs were lysed in 10x radioimmunoprecipitation assay buffer

534   (Millipore), with the concentrated buffer being diluted in distilled water for the cells and

535   in the extracellular vesicle solution for the extracellular vesicles. A total of 30ng of

536   protein was loaded into a 7.5% or 10% polyacrylamide gel (Bio-Rad) in reducing

537   conditions. Following gel electrophoresis, proteins were transferred onto a

538   nitrocellulose membrane (GE Healthcare). Membranes were blocked in 5% bovine

539   serum albumin in tris-buffered saline for 1 hour before being incubated with primary

540   antibodies for ALIX (final concentration 1μg/ml; ab24335; Abcam), CD63 (0.5μg/ml;

541   ab199921; Abcam) or CANX (Calnexin; 1μg/ml; A303-695A; Bethyl Laboratories)

542 overnight at 4°C. Secondary antibody was IRDye 800CW conjugated anti-rabbit IgG

543 (0.2µg/ml; 926-32213; Li-Cor Biosciences). Blots were incubated for 1 hour with

544 secondary antibody and then imaged on the Li-Cor Odyssey Sa (Li-Cor Biosciences).

545 **Proteomics**

546 Watermelon (n=3) cells and matched extracellular vesicles were lysed in10x

547 radioimmunoprecipitation assay buffer (Millipore), as described above for Caco-2 cells

548 and EVs. A total of 600µg of protein – quantified using the Bradford protein assay (Bio-

549 Rad) – was run 5mm into a 10% polyacrylamide gel (Bio-Rad) prior to fixation and

550 staining using Imperial Protein Stain. The excised protein band was dehydrated using

551 acetonitrile then dried via vacuum centrifugation. The proteins in the dried gel piece

552 were reduced with 10mM dithiothreitol then alkylated with 55mM iodoacetamide. The

553 gel piece was washed twice with 25mM ammonium bicarbonate followed by acetonitrile

554 and vacuum centrifugation. Finally, the proteins in the gel were digested in trypsin

555 overnight at 37°C, producing peptides for mass spectrometry analysis. Digested

556 samples were analysed by liquid chromatography coupled-mass spectrometry/mass

557 spectrometry (LC-MS/MS) using an UltiMate® 3000 Rapid Separation LC (Dionex

558 Corporation) coupled to an Orbitrap Elite (Thermo Fisher Scientific, USA) mass

559 spectrometer. Peptide mixtures were separated for 44 min at 300nl/min-1 using a

560 1.7µM Ethylene Bridged Hybrid C18 analytical column (75 mm x 250µm internal

561 diameter; Waters) and 0.1% formic acid in a gradient of 8-33% acetonitrile. Detected

562 peptides were then selected for fragmentation automatically by data dependant

563 analysis. The identified peptides were mapped using Mascot 2.5.1 (Matrix Science UK),

564 to the *Citrullus lanatus* proteome. Mascot 2.5.1 was used with a fragment tolerance of

565 0.60 Da (Monoisotopic), a parent tolerance of 5.0 parts per million (Monoisotopic), fixed

566 modifications of +57 on C (Carbamidomethyl), variable modifications of +16 on M

567 (Oxidation). A maximum of 1 missed cleavage was permitted. Data were validated

568 using Scaffold (Proteome Software, USA), employing the following thresholds: 95%

569 protein identification certainty, 1 for the minimum number of unique peptides mapping

570 to each protein, and 80% peptide identification certainty.

571 **DNA Analysis**

572 DNA was extracted from watermelon (n=3) cells and matched EVs using the ISOLATE

573 II Plant DNA Kit (Bioline) according the manufacturer's instructions. Briefly, watermelon

574 cells were ground into a powder using a pestle and mortar with the aid of liquid

575 nitrogen. Both cells and EVs were lysed using Lysis Buffer PA2. Following DNA

576 extraction, primers towards actin-7 (Forward: 5'-ATGTTCACAACCACTGCCGAACG-3'

577 , Reverse: 5'-AATGAGGGATGGCTGGAAAAGAACTT-3'), rbcL (Forward: 5'-

578 ATGAGTTGTAGGGAGGGACTTATGTCACC'3', Reverse: 5'-

579 GATTTTCTTCTCCAGGAACAGGCTCG-3') and ccmFn (Forward: 5'-

580 CCGGCCATAGGTTCGAATCCTG-3', Reverse: 5'-CCGGCCATAGGTTCGAATCCTG-

581 3') were used to amplify nuclear, plastid and mitochondrial specific DNA respectively

582 from equal amounts of starting DNA using the Fast Cycling PCR Kit (Qiagen). PCR

583 products were run on a 2% agarose gel containing GelRed (Biotium) for band

584 visualisation. Densitometry was conducted using the ImageStudio lite (Li-Cor). The

585 value of any non-specific amplification in negative controls was removed from all

586 densitometry values for the respective primer's product.

587 **Bioinformatics analysis**

588 *Oryza sativa* miRNAs were aligned with published watermelon miRNAs using the blastn

589 mode of BLAST, with those miRNAs with <2 mismatches along the length of the

590 miRNA (i.e. <10% deviation from the watermelon sequence) being considered

591 homologous. T-Coffee Multiple Sequence Alignment was used to create a phylogenetic

26

592   tree of watermelon miRNA sequences. Prediction of miRNA targets was carried out

593   using psRNAtarget [76] using the *Citrullus lanatus* (watermelon), transcript, Cucurbit

594   Genomics Database, version 1[77]. FASTA sequences for watermelon proteins were

595   procured from the Cucurbit Genome Database [77] and were aligned with those from

596   other plant species and humans using the blastp mode of BLAST. An alignment was

597   considered to predict a homolog if the query cover was at least 70%, with 50% identity

598   within this region. In order to predict the subcellular location of EV biogenesis, the

599   known/annotated subcellular localisation of watermelon EV proteins was obtained from

600   the Cucurbit Genome Database[77]. The presence of motifs required for sorting into

601   different subcellular locations was also used to predict subcellular localisation using the

602   CELLO software[78]. Alignment was also performed to the proteome of watermelon

603   chromoplasts[50], the late endosome/MVB proteome of *Arabidopsis thaliana* [51] and

604   transcriptomics data from ripening watermelon fruit [52]. *Arabidopsis thaliana* MVB data

605   was used as no watermelon MVB proteome currently exists in the literature.

606   Hierarchical clustering analysis and principal components analysis was performed

607   using the ClustVis R package [79]. Proteins and predicted miRNA targets were analysed

608   for pathway overrepresentation against the whole watermelon proteome using the

609   Bonferroni test; adjusted p-values of <0.05 were considered significant. This procedure

610   was carried out using the Cucurbit Genome Database.

611   **Statistical analysis**

612   All statistical analysis was performed on GraphPad Prism 8, unless otherwise stated.

613   All measurements reported are on distinct samples. No samples were measured more

614   than once for the same parameter, except where technical replicates were taken. In the

615   case of technical replicates, the mean of these replicates is reported. The individual

616   statistical tests are given in the relevant methods and figures. In brief, all statistical tests

617   on continuous variables between two groups were analysed using the Mann-Whitney

618   test. When more than two groups were compared over time, a two-way ANOVA with

619   Sidak's multiple comparisons test was used. Two-sided tests were used for all

620   analyses.

Data availability

622   The proteomics and miRNA qPCR array data that support the findings of this study are

623   available in Vesiclepedia (http://microvesicles.org/index.html) with the identifier

624   currently pending. We will provide the identifier as soon as it is available. Furthermore,

625   The authors declare that the proteomics, miRNA qPCR array and miRNA predicted

626   target data supporting the findings of this study are also available within the

627   supplementary information files.

Acknowledgements

References

633   1   Brown, L., Wolf, J. M., Prados-Rosales, R. & Casadevall, A. Through the wall:
634   extracellular vesicles in Gram-positive bacteria, mycobacteria and fungi. *Nature*
635   *Reviews Microbiology* **13**, 620-630, doi:10.1038/nrmicro3480 (2015).
636   2   van Niel, G., D'Angelo, G. & Raposo, G. Shedding light on the cell biology of
637   extracellular vesicles. *Nature Reviews Molecular Cell Biology* **19**, 213-228,
638   doi:10.1038/nrm.2017.125 (2018).
639   3   Kosaka, N. *et al.* Secretory Mechanisms and Intercellular Transfer of MicroRNAs in
640   Living Cells. *Journal of Biological Chemistry* **285**, 17442-17452,
641   doi:10.1074/jbc.M110.107821 (2010).
642   4   Mittelbrunn, M. *et al.* Unidirectional transfer of microRNA-loaded exosomes from T cells
643   to antigen-presenting cells. *Nature Communications* **2**, doi:10.1038/ncomms1285
644   (2011).
645   5   Valadi, H. *et al.* Exosome-mediated transfer of mRNAs and microRNAs is a novel
646   mechanism of genetic exchange between cells. *Nat Cell Biol* **9**, 654-659, doi:ncb1596
647   [pii]

648   10.1038/ncb1596 (2007).

649 6   Rutter, B. D. & Innes, R. W. Extracellular Vesicles Isolated from the Leaf Apoplast Carry
650   Stress-Response Proteins. P*lant Physiology* 1**73,** 728-741, doi:10.1104/pp.16.01253
651   (2017).
652 7   Deng, Z. *et al.* Broccoli-Derived Nanoparticle Inhibits Mouse Colitis by Activating
653   Dendritic Cell AMP-Activated Protein Kinase. M*ol Ther* 2**5,** 1641-1654,
654   doi:10.1016/j.ymthe.2017.01.025 (2017).
655 8   Mu, J. Y. *et al.* Interspecies communication between plant and mouse gut host cells
656   through edible plant derived exosome-like nanoparticles. M*olecular Nutrition & Food
657   Research* 5**8,** 1561-1573, doi:10.1002/mnfr.201300729 (2014).
658 9   Zhang, M. *et al.* Edible ginger-derived nanoparticles: A novel therapeutic approach for
659   the prevention and treatment of inflammatory bowel disease and colitis-associated
660   cancer. B*iomaterials* 1**01,** 321-340, doi:10.1016/j.biomaterials.2016.06.018 (2016).
661 10   Zhang, M., Wang, X., Han, M. K., Collins, J. F. & Merlin, D. Oral administration of
662   ginger-derived nanolipids loaded with siRNA as a novel approach for efficient siRNA
663   drug delivery to treat ulcerative colitis. N*anomedicine (Lond)* 1**2,** 1927-1943,
664   doi:10.2217/nnm-2017-0196 (2017).
665 11   Ju, S. W. *et al.* Grape Exosome-like Nanoparticles Induce Intestinal Stem Cells and
666   Protect Mice From DSS-Induced Colitis. M*olecular Therapy* 2**1,** 1345-1357,
667   doi:10.1038/mt.2013.64 (2013).
668 12   Pérez-Bermúdez, P., Blesa, J., Soriano, J. M. & Marcilla, A. Extracellular vesicles in
669   food: Experimental evidence of their secretion in grape fruits. E*ur J Pharm Sci* 9**8,** 40-
670   50, doi:10.1016/j.ejps.2016.09.022 (2017).
671 13   Wang, B. M. *et al.* Targeted Drug Delivery to Intestinal Macrophages by Bioactive
672   Nanovesicles Released from Grapefruit. M*olecular Therapy* 2**2,** 522-534,
673   doi:10.1038/mt.2013.190 (2014).
674 14   Raimondo, S. *et al.* Citrus limon-derived nanovesicles inhibit cancer cell proliferation
675   and suppress CML xenograft growth by inducing TRAIL-mediated cell death.
676   O*ncotarget* 6, 19514-19527, doi:10.18632/oncotarget.4004 (2015).
677 15   Regente, M. *et al.* Vesicular fractions of sunflower apoplastic fluids are associated with
678   potential exosome marker proteins. F*ebs Letters* 5**83,** 3363-3366,
679   doi:10.1016/j.febslet.2009.09.041 (2009).
680 16   Xiao, J. *et al.* Identification of exosome-like nanoparticle-derived microRNAs from 11
681   edible fruits and vegetables. P*eerJ* 6**,** e5186, doi:10.7717/peerj.5186 (2018).
682 17   Raposo, G. *et al.* B lymphocytes secrete antigen-presenting vesicles. J*ournal of
683   Experimental Medicine* 1**83,** 1161-1172, doi:10.1084/jem.183.3.1161 (1996).
684 18   Futter, C. E., Pearse, A., Hewlett, L. J. & Hopkins, C. R. Multivesicular endosomes
685   containing internalized EGF-EGF receptor complexes mature and then fuse directly with
686   lysosomes. J*ournal of Cell Biology* 1**32,** 1011-1023, doi:10.1083/jcb.132.6.1011 (1996).
687 19   Donker, R. B. *et al.* The expression profile of C19MC microRNAs in primary human
688   trophoblast cells and exosomes. M*olecular Human Reproduction* 1**8,** 417-424,
689   doi:10.1093/molehr/gas013 (2012).
690 20   Van Niel, G. *et al.* Intestinal epithelial cells secrete exosome–like vesicles.
691   G*astroenterology* 1**21,** 337-349, doi:http://dx.doi.org/10.1053/gast.2001.26263 (2001).
692 21   Hunter, M. P. *et al.* Detection of microRNA Expression in Human Peripheral Blood
693   Microvesicles. P*los One* 3**,** 11, doi:10.1371/journal.pone.0003694 (2008).
694 22   Heijnen, H. F. G., Schiel, A. E., Fijnheer, R., Geuze, H. J. & Sixma, J. J. Activated
695   platelets release two types of membrane vesicles: Microvesicles by surface shedding
696   and exosomes derived from exocytosis of multivesicular bodies and alpha-granules.
697   B*lood* 9**4,** 3791-3799 (1999).
698 23   Villarroya-Beltri, C. *et al.* Sumoylated hnRNPA2B1 controls the sorting of miRNAs into
699   exosomes through binding to specific motifs. N*ature Communications* 4**,** 10,
700   doi:10.1038/ncomms3980 (2013).
701 24   Moreno-Gonzalo, O., Fernandez-Delgado, I. & Sanchez-Madrid, F. Post-translational
702   add-ons mark the path in exosomal protein sorting. C*ellular and Molecular Life Sciences
703   *7**5,** 1-19, doi:10.1007/s00018-017-2690-y (2018).

704 25 Holme, P. A., Brosstad, F. & Solum, N. O. The difference between platelet and plasma
705   FXIII used to study the mechanism of platelet microvesicle formation. T*hrombosis and*
706   *Haemostasis* 7**0,** 681-686 (1993).
707 26 Hristov, M., Erl, W., Linder, S. & Weber, P. C. Apoptotic bodies from endothelial cells
708   enhance the number and initiate the differentiation of human endothelial progenitor cells
709   in vitro. B*lood* 1**04,** 2761-2766 (2004).
710 27 Cotter, T. G., Lennon, S. V., Glynn, J. M. & Green, D. R. Microfilament-disrupting
711   agents prevent the formation of apoptotic bodies in tumour cells undergoing apoptosis.
712   C*ancer Research* 5**2,** 997-1005 (1992).
713 28 Jiang, L. *et al.* Determining the contents and cell origins of apoptotic bodies by flow
714   cytometry. S*cientific Reports* 7**,** doi:10.1038/s41598-017-14305-z (2017).
715 29 An, Q. L., Huckelhoven, R., Kogel, K. H. & Van Bel, A. J. E. Multivesicular bodies
716   participate in a cell wall-associated defence response in barley leaves attacked by the
717   pathogenic powdery mildew fungus. C*ellular Microbiology* 8**,** 1009-1019,
718   doi:10.1111/j.1462-5822.2006.00683.x (2006).
719 30 Baldrich, P. *et al.* Plant Extracellular Vesicles Contain Diverse Small RNA Species and
720   Are Enriched in 10-to 17-Nucleotide "Tiny" RNAs. P*lant Cell* 3**1,** 315-324,
721   doi:10.1105/tpc.18.00872 (2019).
722 31 Cai, Q. *et al.* Plants send small RNAs in extracellular vesicles to fungal pathogen to
723   silence virulence genes. S*cience* 3**60,** 1126-1129, doi:10.1126/science.aar4142 (2018).
724 32 Rutter, B. D. & Innes, R. W. Extracellular vesicles as key mediators of plant-microbe
725   interactions. C*urrent Opinion in Plant Biology* 4**4,** 16-22, doi:10.1016/j.pbi.2018.01.008
726   (2018).
727 33 Regente, M., Monzon, G. C. & de la Canal, L. Phospholipids are present in extracellular
728   fluids of imbibing sunflower seeds and are modulated by hormonal treatments. J*ournal*
729   *of Experimental Botany* 5**9,** 553-562, doi:10.1093/jxb/erm329 (2008).
730 34 Gonorazky, G., Laxalt, A. M., Testerink, C., Munnik, T. & De La Canal, L.
731   Phosphatidylinositol 4-phosphate accumulates extracellularly upon xylanase treatment
732   in tomato cell suspensions. P*lant Cell and Environment* 3**1,** 1051-1062,
733   doi:10.1111/j.1365-3040.2008.01818.x (2008).
734 35 Regente, M., Pinedo, M., Elizalde, M. & de la Canal, L. Apoplastic exosome-like
735   vesicles A new way of protein secretion in plants? P*lant Signaling & Behavior* 7**,** 544-
736   546, doi:10.4161/psb.19675 (2012).
737 36 Baietti, M. F. *et al.* Syndecan-syntenin-ALIX regulates the biogenesis of exosomes.
738   N*ature Cell Biology* 1**4,** 677-685, doi:10.1038/ncb2502 (2012).
739 37 Iavello, A. *et al.* Role of Alix in miRNA packaging during extracellular vesicle biogenesis.
740   I*nternational Journal of Molecular Medicine* 3**7,** 958-966, doi:10.3892/ijmm.2016.2488
741   (2016).
742 38 Haraszti, R. A. *et al.* High-resolution proteomic and lipidomic analysis of exosomes and
743   microvesicles from different cell sources. J*ournal of Extracellular Vesicles* 5**,**
744   doi:10.3402/jev.v5.32570 (2016).
745 39 Théry, C. *et al.* Minimal information for studies of extracellular vesicles 2018
746   (MISEV2018): a position statement of the International Society for Extracellular Vesicles
747   and update of the MISEV2014 guidelines. J*ournal of Extracellular Vesicles* 8**,** 1535750,
748   doi:10.1080/20013078.2018.1535750 (2019).
749 40 Squadrito, M. L. *et al.* Endogenous RNAs Modulate MicroRNA Sorting to Exosomes and
750   Transfer to Acceptor Cells. C*ell Reports* 8**,** 1432-1446, doi:10.1016/j.celrep.2014.07.035
751   (2014).
752 41 Kim, D. K. *et al.* EVpedia: a community web portal for extracellular vesicles research.
753   B*ioinformatics* 3**1,** 933-939, doi:10.1093/bioinformatics/btu741 (2015).
754 42 Kalra, H. *et al.* Vesiclepedia: A Compendium for Extracellular Vesicles with Continuous
755   Community Annotation. P*los Biology* 1**0,** doi:10.1371/journal.pbio.1001450 (2012).
756 43 Lindquist, E., Solymosi, K. & Aronsson, H. Vesicles Are Persistent Features of Different
757   Plastids. T*raffic* 1**7,** 1125-1138, doi:10.1111/tra.12427 (2016).

44   Westphal, S., Soll, J. & Vothknecht, U. C. A vesicle transport system inside chloroplasts. F*ebs Letters* 5**06,** 257-261, doi:10.1016/s0014-5793(01)02931-3 (2001).

45   Morre, D. J., Sellden, G., Sundqvist, C. & Sandelius, A. S. STROMAL LOW-TEMPERATURE COMPARTMENT DERIVED FROM THE INNER MEMBRANE OF THE CHLOROPLAST ENVELOPE. P*lant Physiology* 9**7,** 1558-1564, doi:10.1104/pp.97.4.1558 (1991).

46   Zhang, L., Kato, Y., Otters, S., Vothknecht, U. C. & Sakamoto, W. Essential Role of VIPP1 in Chloroplast Envelope Maintenance in Arabidopsis. P*lant Cell* 2**4,** 3695-3707, doi:10.1105/tpc.112.103606 (2012).

47   Aseeva, E. *et al.* Vipp1 is required for basic thylakoid membrane formation but not for the assembly of thylakoid protein complexes. P*lant Physiology and Biochemistry* 4**5,** 119-128, doi:10.1016/j.plaphy.2007.01.005 (2007).

48   Kroll, D. *et al.* VIPP1, a nuclear gene of Arabidopsis thaliana essential for thylakoid membrane formation. P*roceedings of the National Academy of Sciences of the United States of America* 9**8,** 4238-4242, doi:10.1073/pnas.061500998 (2001).

49   Caiola, M. G. & Canini, A. Ultrastructure of chromoplasts and other plastids in Crocus sativus L. (Iridaceae). P*lant Biosystems* 1**38,** 43-52, doi:10.1080/11263500410001684116 (2004).

50   Wang, Y. Q. *et al.* Proteomic analysis of chromoplasts from six crop species reveals insights into chromoplast function and development. J*ournal of Experimental Botany* 6**4,** 949-961, doi:10.1093/jxb/ers375 (2013).

51   Heard, W., Sklenar, J., Tome, D. F. A., Robatzek, S. & Jones, A. M. E. Identification of Regulatory and Cargo Proteins of Endosomal and Secretory Pathways in Arabidopsis thaliana by Proteomic Dissection. M*olecular & Cellular Proteomics* 1**4,** 1796-1813, doi:10.1074/mcp.M115.050286 (2015).

52   Zhu, Q. L. *et al.* Comparative transcriptome analysis of two contrasting watermelon genotypes during fruit development and ripening. B*mc Genomics* 1**8,** doi:10.1186/s12864-016-3442-3 (2017).

53   Thery, C., Amigorena, S., Raposo, G. & Clayton, A. Isolation and characterization of exosomes from cell culture supernatants and biological fluids. C*urrent protocols in cell biology* C**hapter 3,** Unit 3.22-Unit 23.22, doi:10.1002/0471143030.cb0322s30 (2006).

54   Webber, J. & Clayton, A. How pure are your vesicles? J*ournal of Extracellular Vesicles* 2**,** 19861, doi:10.3402/jev.v2i0.19861 (2013).

55   Witwer, K. W. *et al.* Standardization of sample collection, isolation and analysis methods in extracellular vesicle research. J*ournal of extracellular vesicles* 2**,** doi:10.3402/jev.v2i0.20360 (2013).

56   Thyssen, G., Svab, Z. & Maliga, P. Cell-to-cell movement of plastids in plants. P*roceedings of the National Academy of Sciences of the United States of America* 1**09,** 2439-2443, doi:10.1073/pnas.1114297109 (2012).

57   Bobik, K. & Burch-Smith, T. M. Chloroplast signaling within, between and beyond cells. F*rontiers in Plant Science* 6**,** doi:10.3389/fpls.2015.00781 (2015).

58   Nielsen, M. E., Feechan, A., Boehlenius, H., Ueda, T. & Thordal-Christensen, H. Arabidopsis ARF-GTP exchange factor, GNOM, mediates transport required for innate immunity and focal accumulation of syntaxin PEN1. P*roceedings of the National Academy of Sciences of the United States of America* 1**09,** 11443-11448, doi:10.1073/pnas.1117596109 (2012).

59   Liu, X. *et al.* Identification and transcript profiles of citrus growth-regulating factor genes involved in the regulation of leaf and fruit development. M*olecular Biology Reports* 4**3,** 1059-1067, doi:10.1007/s11033-016-4048-1 (2016).

60   Wang, L. *et al.* miR396-targeted AtGRF transcription factors are required for coordination of cell division and differentiation during leaf development in Arabidopsis. J*ournal of Experimental Botany* 6**2,** 761-773, doi:10.1093/jxb/erq307 (2011).

61   Wang, L., Du, H. Y. & Wuyun, T. N. Genome-Wide Identification of MicroRNAs and Their Targets in the Leaves and Fruits of Eucommia ulmoides Using High-Throughput Sequencing. F*rontiers in Plant Science* 7**,** 15, doi:10.3389/fpls.2016.01632 (2016).

813   62   Cao, D. Y. *et al.* Regulations on growth and development in tomato cotyledon, flower
814   and fruit via destruction of miR396 with short tandem target mimic. P*lant Science* 2**47,**
815   1-12, doi:10.1016/j.plantsci.2016.02.012 (2016).
816   63   Csukasi, F. *et al.* Two strawberry miR159 family members display developmental-
817   specific expression patterns in the fruit receptacle and cooperatively regulate Fa-
818   GAMYB. N*ew Phytologist* 1**95,** 47-57, doi:10.1111/j.1469-8137.2012.04134.x (2012).
819   64   da Silva, E. M. *et al.* microRNA159-targeted SlGAMYB transcription factors are required
820   for fruit set in tomato. P*lant Journal* 9**2,** 95-109, doi:10.1111/tpj.13637 (2017).
821   65   Palatnik, J. F. *et al.* Sequence and expression differences underlie functional
822   specialization of Arabidopsis microRNAs miR159 and miR319. D*ev Cell* 1**3,** 115-125,
823   doi:10.1016/j.devcel.2007.04.012 (2007).
824   66   Allen, R. S. *et al.* Genetic analysis reveals functional redundancy and the major target
825   genes of the Arabidopsis miR159 family. P*roceedings of the National Academy of*
826   *Sciences of the United States of America* 1**04,** 16371-16376,
827   doi:10.1073/pnas.0707653104 (2007).
828   67   Stegemann, S. & Bock, R. Exchange of Genetic Material Between Cells in Plant Tissue
829   Grafts. S*cience* 3**24,** 649-651, doi:10.1126/science.1170397 (2009).
830   68   Molnar, A. *et al.* Small Silencing RNAs in Plants Are Mobile and Direct Epigenetic
831   Modification in Recipient Cells. S*cience* 3**28,** 872-875, doi:10.1126/science.1187959
832   (2010).
833   69   Fragoso, V., Goddard, H., Baldwin, I. T. & Kim, S. G. A simple and efficient
834   micrografting method for stably transformed Nicotiana attenuata plants to examine
835   shoot-root signaling. P*lant Methods* 7**,** 8, doi:10.1186/1746-4811-7-34 (2011).
836   70   Melnyk, C. W., Molnar, A., Bassett, A. & Baulcombe, D. C. Mobile 24 nt Small RNAs
837   Direct Transcriptional Gene Silencing in the Root Meristems of Arabidopsis thaliana.
838   C*urrent Biology* 2**1,** 1678-1683, doi:10.1016/j.cub.2011.08.065 (2011).
839   71   Buhtz, A., Pieritz, J., Springer, F. & Kehr, J. Phloem small RNAs, nutrient stress
840   responses, and systemic mobility. B*mc Plant Biology* 1**0,** 13, doi:10.1186/1471-2229-
841   10-64 (2010).
842   72   Wang, J., Jiang, L. B. & Wu, R. L. Plant grafting: how genetic exchange promotes
843   vascular reconnection. N*ew Phytologist* 2**14,** 56-65, doi:10.1111/nph.14383 (2017).
844   73   Pina, A., Errea, P. & Martens, H. J. Graft union formation and cell-to-cell communication
845   via plasmodesmata in compatible and incompatible stem unions of Prunus spp. S*cientia*
846   *Horticulturae* 1**43,** 144-150, doi:10.1016/j.scienta.2012.06.017 (2012).
847   74   Van Deun, J. *et al.* EV-TRACK: transparent reporting and centralizing knowledge in
848   extracellular vesicle research. N*ature Methods* 1**4,** 228-232, doi:10.1038/nmeth.4185
849   (2017).
850   75   Li, A. L. & Mao, L. Evolution of plant microRNA gene families. C*ell Research* 1**7,** 212-
851   218, doi:10.1038/sj.cr.7310113 (2007).
852   76   Dai, X. B. & Zhao, P. X. psRNATarget: a plant small RNA target analysis server. N*ucleic*
853   *Acids Research* 3**9,** W155-W159, doi:10.1093/nar/gkr319 (2011).
854   77   Feilab. '*Cucurbit Genome Database',* <http://cucurbitgenomics.org/> (2017).
855   78   Yu, C.-S., Chen, Y.-C., Lu, C.-H. & Hwang, J.-K. Prediction of protein subcellular
856   localization. P*roteins: Structure, Function, and Bioinformatics* 6**4,** 643-651,
857   doi:10.1002/prot.21018 (2006).
858   79   Metsalu, T. & Vilo, J. ClustVis: a web tool for visualizing clustering of multivariate data
859   using Principal Component Analysis and heatmap. N*ucleic Acids Research* 4**3,** W566-
860   W570, doi:10.1093/nar/gkv468 (2015).
861